

Supplementary Information

Template-free fabrication of partially aligned (100) fcc thin film colloidal crystals

Midhun Joy, Tanyakorn Muangnapoh, Mark A. Snyder*, and James F. Gilchrist*

Department of Chemical and Biomolecular Engineering, Lehigh University,
Bethlehem, PA, 18015, USA

* Co-corresponding authors: gilchrist@lehigh.edu, Tel: +1 610 758 4781;
snyder@lehigh.edu, Tel: +1 610 758 6834; Fax: +1 610 758 5057

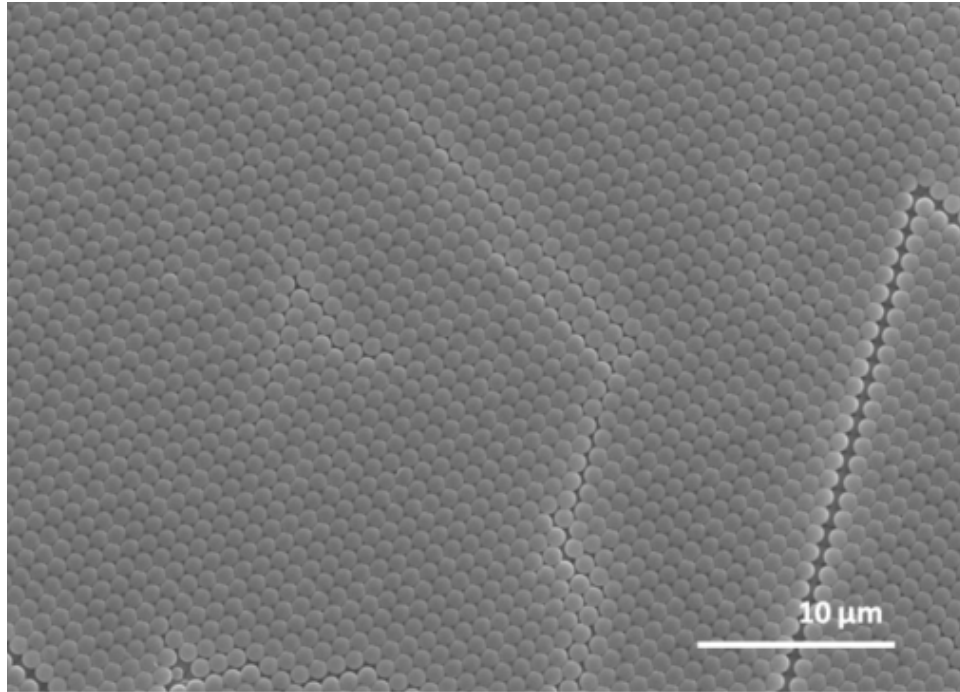


Fig. S1 Representative SEM of a region of the top surface of a colloidal crystal film prepared by vibration assisted convective assembly showing rhcp packing co-existing with square-packed regions.

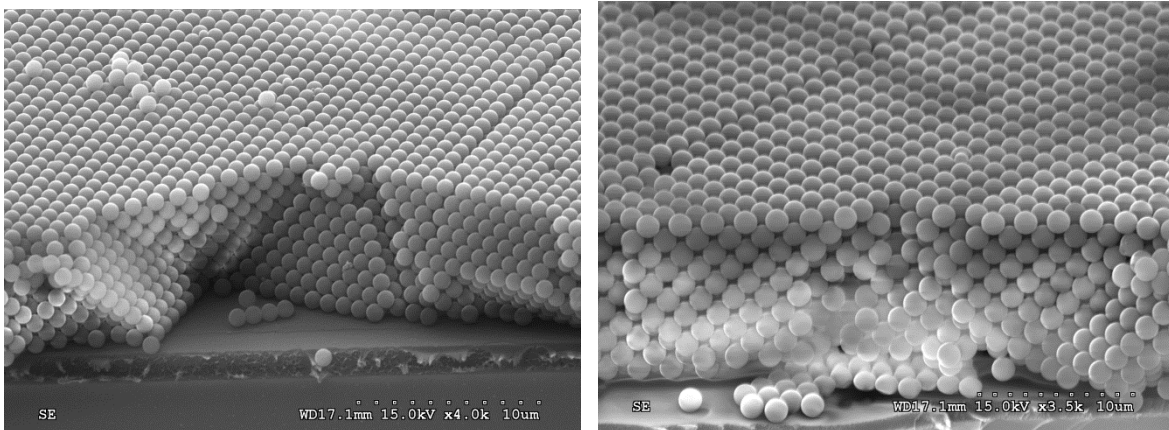


Fig. S2 Cross-sectional images of coexisting (left) rhcp and (right) square-packed domains within a colloidal crystal film prepared by vibration assisted convective assembly.

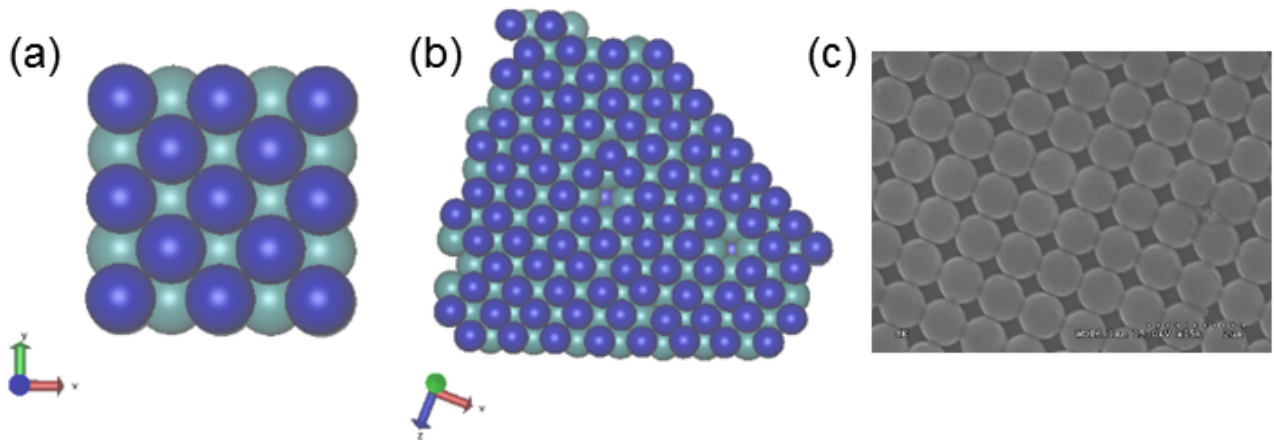


Fig. S3 Comparison of planar views of as-obtained square-packed structure with that of (100) fcc structure (a) Ideal (100) fcc structure generated by VMD (b) VMD rendering of actual particles constituting square-packed region (c) SEM image of the sample

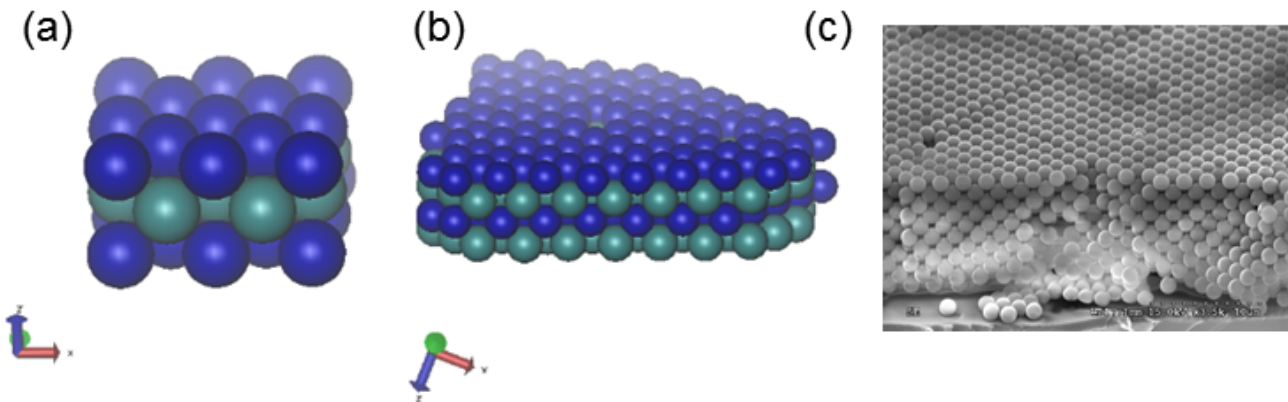
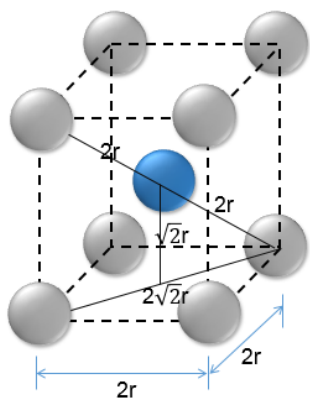


Fig. S4 Comparison of cross-sectional views of as-obtained square-packed structure with that of (100) fcc structure (a) Ideal (100) fcc structure generated by VMD (b) VMD rendering of actual particles constituting square-packing (c) SEM image of the sample



For square-packed structure obtained with $0.93 \mu\text{m}$ PS particles, the distance between consecutive layers, averaged over multiple unit cells were found to be $0.64 \mu\text{m}$, which matches with the theoretical value of $0.657 \mu\text{m}$ with an error of 2 % owing to the optical resolution limit of the instrument. Also, the packing fraction of actual structure obtained by CLSM analysis was found to be 76 %, which is almost equal to that of the fcc structure.

Fig. S5 Schematic of a (100) fcc unit cell

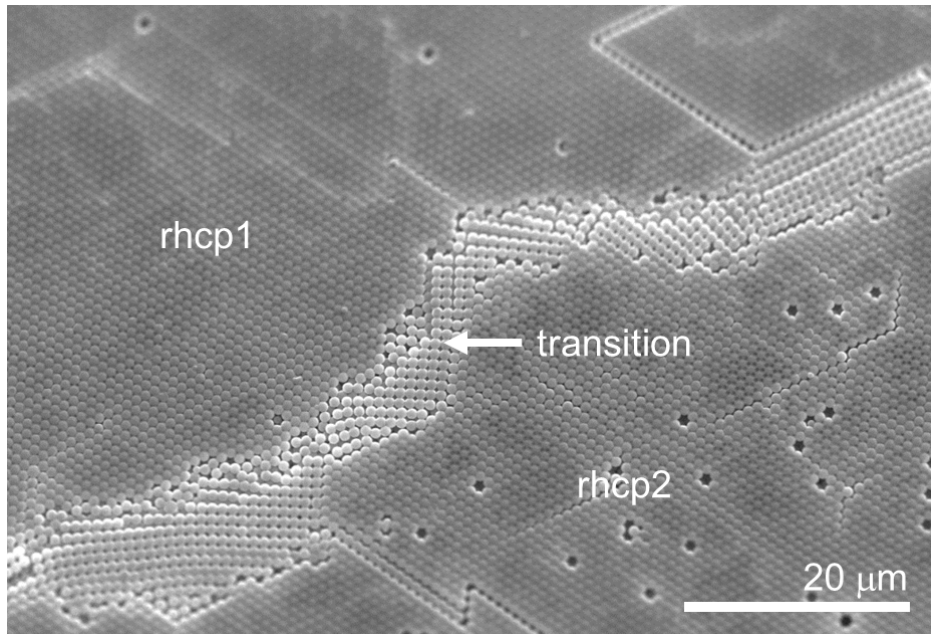


Fig. S6 Square packing (i.e., (100) fcc domains) observed at the transition (arrow) between hexagonally packed regions (hcp1, hcp2) of different thickness.

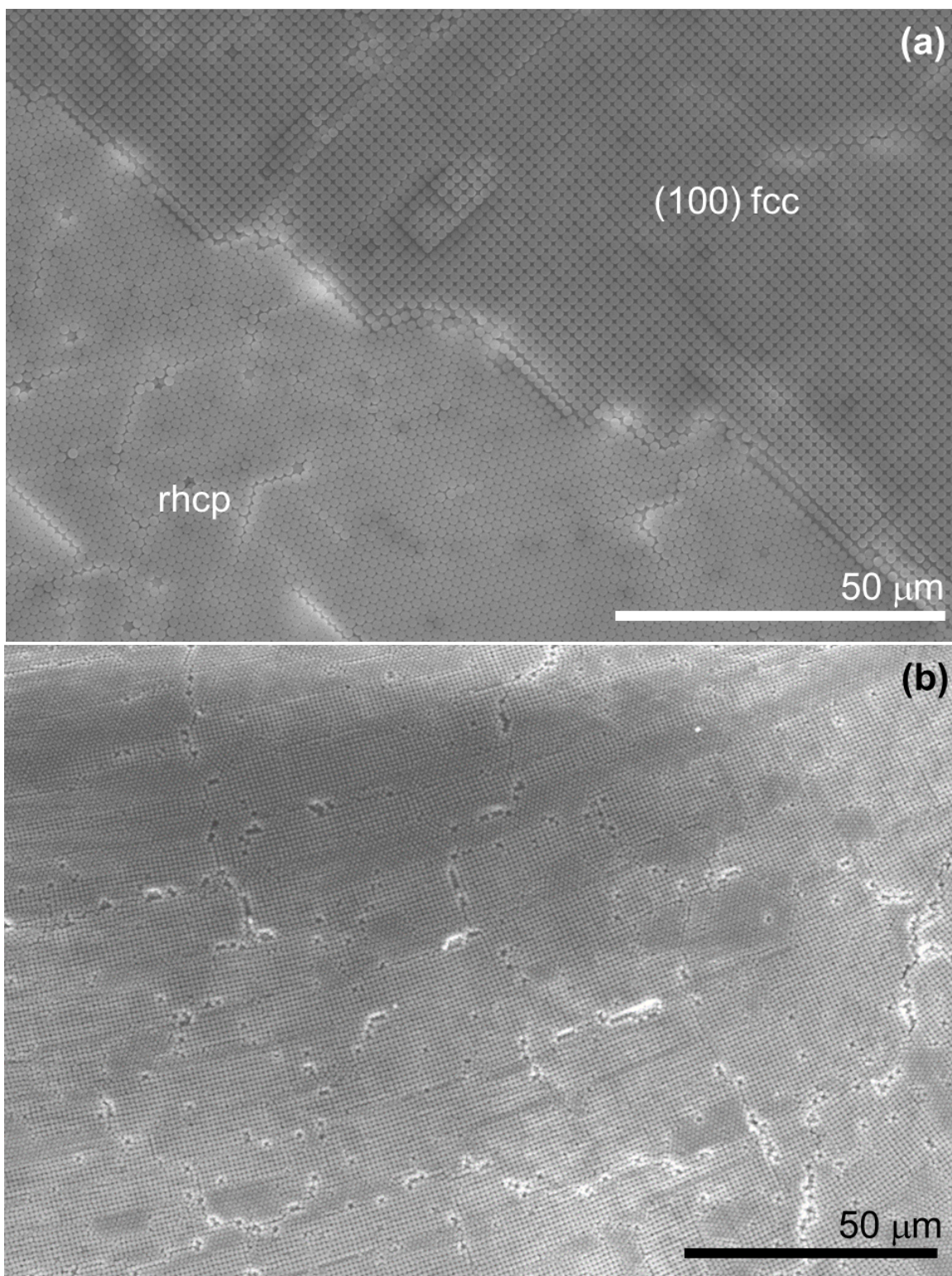


Fig. S7 (100) fcc domains realized by vibration-assisted convective deposition of (a) 1.5 μm polystyrene particles and (b) 1 μm silica particles.

Image Analysis Procedure:

The colloidal-crystal samples assembled on the substrate of dimensions 5 cm x 4 cm using the outlined procedure were analyzed under a Confocal laser scanning microscope (CLSM) at 100x magnification. Multiple confocal scans of the sample were necessitated owing to the large dimensions of the sample and performed both in the lateral direction (direction of deposition) and longitudinal direction (perpendicular to deposition direction). The image stack thus obtained were analyzed using the particle tracking algorithm developed by John C. Crocker and Eric R. Weeks¹ to identify the centroid locations of the particles. The following calculations were then performed on the particles identified in the scanned images, a representative reconstruction of various steps given by Figures S8,S10 on the basis of a sample image.

1. Identification of particles containing four and six nearest neighbors

This is achieved by first scaling the particle co-ordinates of the features present in a frame in terms of the particle diameter. A spherical cavity with radii of 0.8 and 1.2 particle-diameter units was assumed around each particle, followed by grouping of particles which have 6 and 4 nearest neighbors (defined as the particles whose centroid lies within the above assumed spherical cavity). Based on the number of nearest neighbors (NN), the color scheme as shown in Figure S8b is used to represent the various types of features.

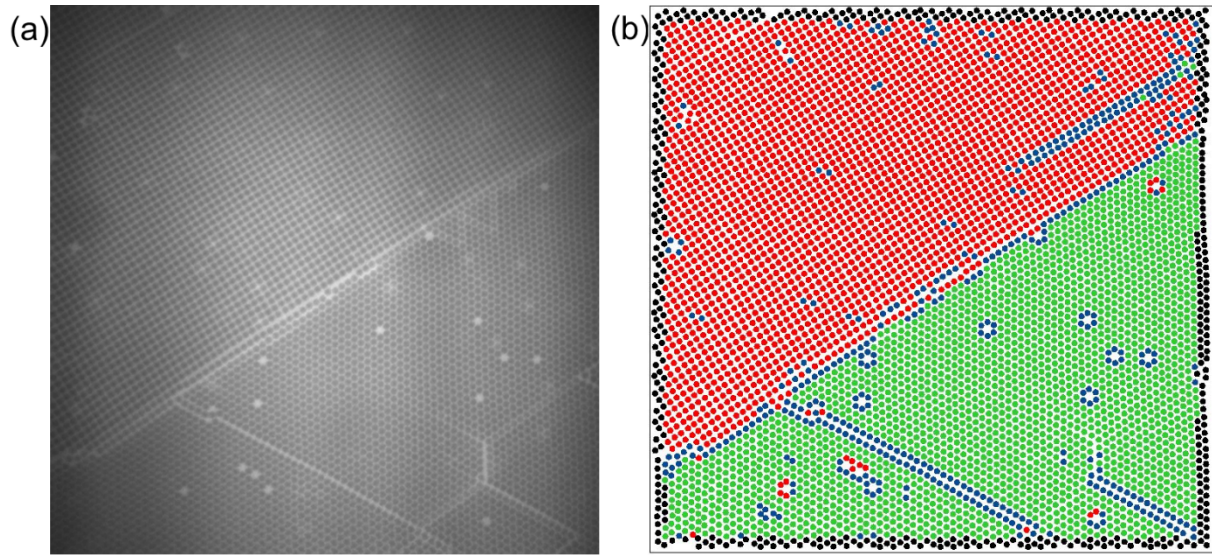


Fig. S8 Tracking of particle centroid locations and identification of number of nearest neighbors (a) Representative confocal image with both square and hexagonal packed regions. (b) Reconstructed image with particles grouped into square-packed regions with four nearest neighbors (red), hexagonally-packed regions with six nearest neighbors (green), particles with neither four nor six nearest neighbors (blue) and particles at the boundary of the frame (black)

2. Recalculation to account for the inaccurate estimation of the particle type

This was necessitated as the absence of particles in some locations, either due to a defect in packing during the colloidal-crystal assembly or being out of focus during the confocal scans results in a void space in what is actually a hexagonal or a square domain. This results in an inaccurate estimation of the particle type if its description is based only on its number of nearest neighbors and can be observed in Figure S8b as isolated green-color particles in the square-packed region or isolated red-colored particles around a void in the hexagonally-packed region.

This inaccuracy in the estimation of the particle type is accounted for by using the local-bond order of the particles constituting the rhcp or fcc(100) regions. Local-bond order (ψ) for a particle ' j ' is defined as:

$$\psi_q(r_{jk}) = \frac{1}{N} \sum_{k=1}^N e^{q i \theta(r_{jk})}$$

where N is the number of neighbors for a particle ' j ', ' i ' is the complex conjugate and $\theta(r_{kj})$ denotes the angle between the vector r particles ' j ' and ' k '. A particle with a perfect hexagonal arrangement has six nearest neighbors in its plane, with $N = 6$ and $\theta(r_{kj}) = 60^\circ$ (for $k = 1, 2, 3 \dots 6$), resulting in $\psi_6 = 1$. Similarly, a particle with perfect square arrangement has $\theta(r_{kj}) = 90^\circ$ (for $k = 1, 2, 3, 4$) with $\psi_4 = 1$.

To obtain an estimate of the cut-off values for ψ_6 and ψ_4 which can accurately compartmentalize the particles as belonging to hexagonally-packed and square-packed regions respectively, a sample confocal image was considered which contained almost equal proportions of both packing arrangements (Figure S8a), and particles were classified into groups merely by counting the number of nearest neighbors. Histograms were obtained for $|\psi_6|^2$ (for particles observed to have 6 nearest neighbors) and $|\psi_4|^2$ (for particles with 4 NN), the plots for which are given in Figure S9a.

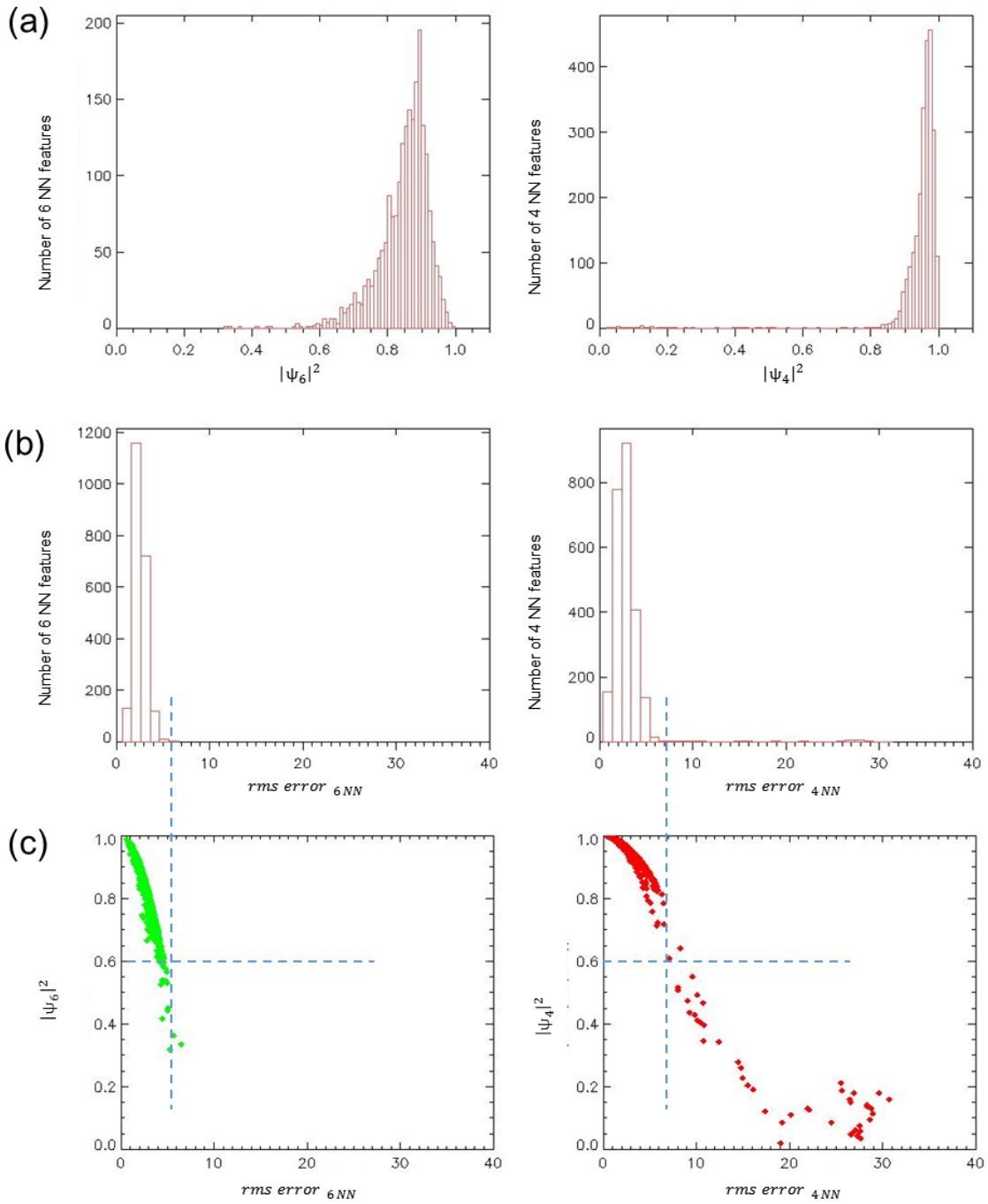


Fig. S9 Calculations to identify the threshold $|\psi_6|$ and $|\psi_4|$ values for 6 NN and 4 NN particles respectively (a) Histograms for $|\psi_6|^2$ (for particles observed to have 6 nearest neighbors) and $|\psi_4|^2$ (for particles with 4 NN) (b) Histograms for 'rms error' for NN and 4 NN particles respectively (c) Plot of $|\psi|^2$ vs 'rms error' for both categories of particles

The histograms in Figure S9a displayed an asymptotic decay for the $|\psi|^2$ values and is not much helpful in defining a threshold- ψ value. This makes it essential to define a modified parameter: 'rms error' to measure how close the particle packing is to the perfect hexagonal or square packing-type (characterized by individual bond angles of 60° and 90° respectively).

The rms error associated with a particle ' j ' having 6 NN is given by:

$$rms\ error_{6\ NN,j} = \sqrt{\frac{1}{6} \sum_{k=1}^6 (\theta_{jk} - 60)^2}$$

Similarly, the rms error associated with a particle ' j ' having 4 NN is given by:

$$rms\ error_{4\ NN,j} = \sqrt{\frac{1}{4} \sum_{k=1}^6 (\theta_{jk} - 90)^2}$$

The rms error values for particles having 6 NN lies in the range of 0 to 6, while that for particles having 4 NN have an upper threshold of 7, barring a few outliers (Figure S9b,c).

This translates to a $|\psi|^2$ value of 0.6, or a $|\psi|$ value of 0.77 for both $|\psi_6|$ and $|\psi_4|$, a threshold chosen so as to capture most of the features of both 6 NN and 4 NN category.

For the particle grouping as described by Figure S8b, a set of recalculation is done for each of the particle based on their ψ values, resulting in the removal of particles with a $|\psi|$ value less than 0.77 from the 6 NN or the 4 NN grouping. The color-coded representation of the particles after the ψ value-based recalculation is depicted by the colored image in Figure S10a, with the particles not satisfying the ψ - criteria added to the group of blue-colored particles.

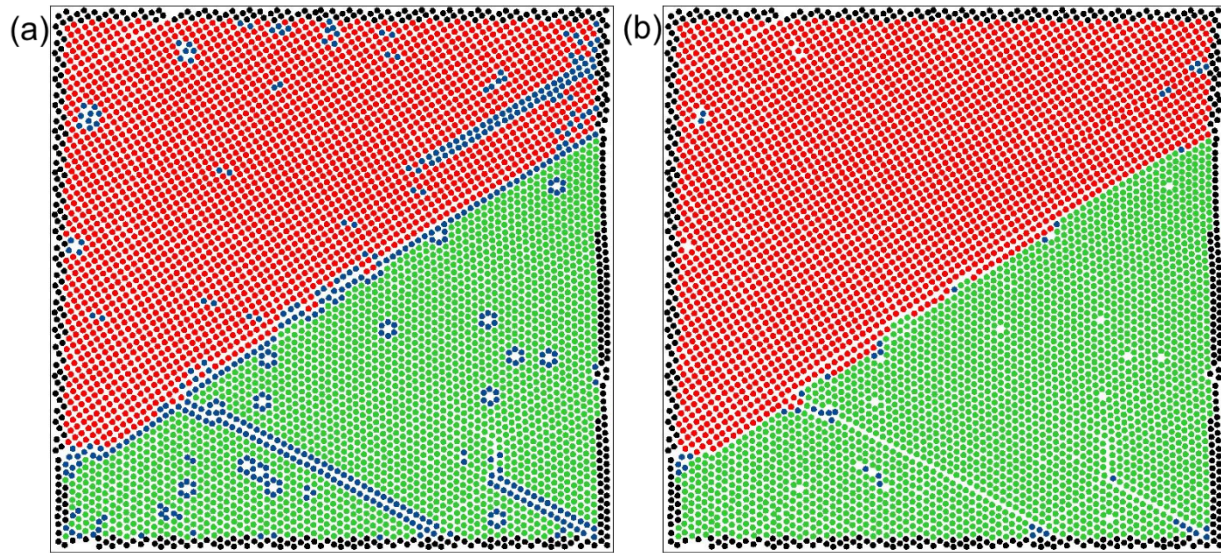


Fig. S10 Modified particle representation after (a) First recalculation based on $|\psi|$ values (b) Second recalculation of blue-colored particles based on its neighboring particles

3. Recalculation to modify the description of blue-colored particles based on the description of its neighbors.

These calculations are done to account for the blue-colored particles, which are usually particles lying at the domain boundaries or associated with a void spaces.

A blue-colored particle is added to the list of particles with 6 NN if:

- (i) The number of neighbors belonging to the 6 NN grouping $>$ Number of neighbors belonging to 4 NN grouping
- (ii) There are at least 2 neighbors belonging to 6 NN grouping with $|\psi_6| \geq 0.77$

Similarly, it is added to the list of particles with 4 NN if:

- (i) The number of neighbors belonging to the 4 NN grouping \geq Number of neighbors belonging to 6 NN grouping
- (ii) There is at least 1 neighbor belonging to 4 NN grouping with $|\psi_4| \geq 0.77$

A pictorial representation of the particle –grouping into 4 NN and 6 NN categories is given by Figure S10b.

4. Identification of (100) fcc domains

A (100) fcc domain represents a grouping of particles belonging to 4 NN category and lying adjacent to each other forming a continuous region. The particle grouping based on the characteristics of its nearest neighbors uses a relaxed criteria of two particle diameters for the scaled centroid co-ordinates. A representational grouping of 4 NN particles into various domains is shown in Figure S11a,b. The typical grouping of 4 NN particles is considered to be a domain only if there are at least 100 particles in the grouping and has at least 10 4 NN particles with $|\psi_4| \geq 0.77$.

5. Calculation of orientation of (100) fcc domains

The calculation procedure for the estimation of cubic-domain orientations is a two-step process, in which the local orientation of the particles are first calculated, which are then averaged to obtain the orientation of the entire domain. For each particle identified as a part of any fcc(100) domain (and actually containing 4 nearest neighbors), the local orientation of the particle is calculated as the average of the bond angles of the particle with each of its four neighbors.

$$\theta_{orient,p}' = \frac{1}{4}(|\theta_{1,p} - 0| + |\theta_{2,p} - 90| + |\theta_{3,p} - 180| + |\theta_{4,p} - 270|)$$

where $\theta_{i,p}$ ($i = 1,2,3,4$) is the bond-angle of 'p' with each of its four neighbors

$$\theta_{orient,p} = \text{modulus}(\theta_{orient,p}, 90)$$

$$\text{if } \theta_{orient,p} > 45, \text{ then } \theta_{orient,p} = 90 - \theta_{orient,p}$$

The orientation of a domain is calculated by averaging the orientation of the individual particles constituting the domain, a representational sketch given in Figure S11b.

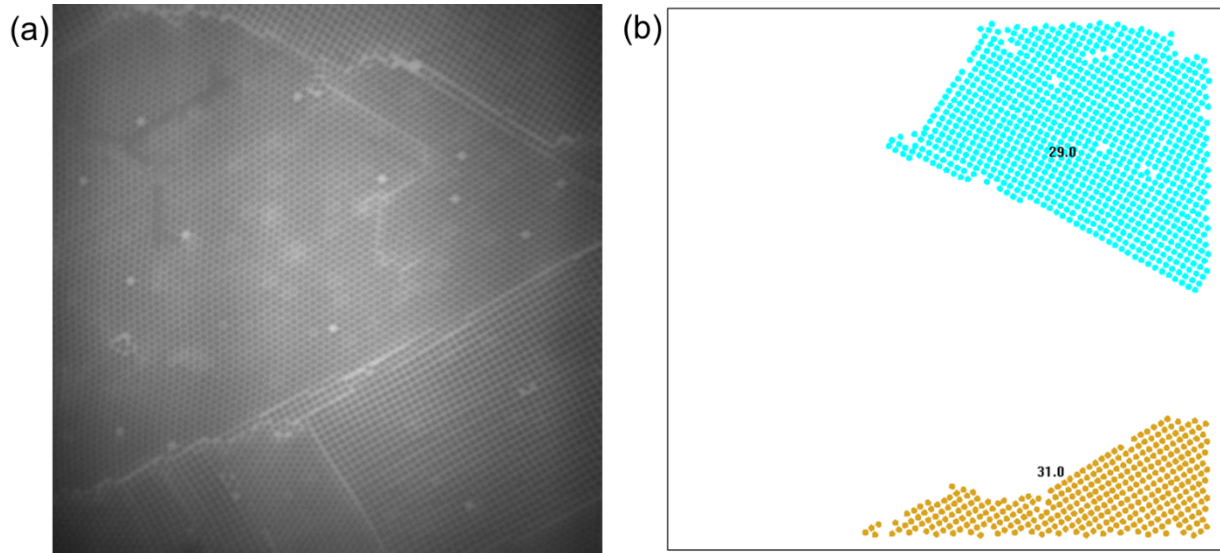


Fig. S11 Grouping of square-packed particles into (100) fcc domains and calculation of the average orientation of these domains

REFERENCES

1. Crocker, J. C. and Weeks, E. R. Particle tracking using IDL; <http://www.physics.emory.edu/~weeks/idl/>.